Irreversible Binding and Activity Control of the 1,2-Diacylglycerol 3-Glucosyltransferase from *Acholeplasma laidlawii* at an Anionic Lipid Bilayer Surface†

Lu Li,[‡,§,||] Patrik Storm,[§,⊥] Olof P. Karlsson,[#] Stefan Berg,[‡,@] and Åke Wieslander*[,⊥]

Department of Biochemistry, Umeå University, Umeå, Sweden, Department of Biochemistry and Chemistry, Biacore AB, Uppsala, Sweden, and Department of Biochemistry and Biophysics, Stockholm University, Stockholm, Sweden

Received March 5, 2003; Revised Manuscript Received June 19, 2003

ABSTRACT: 1,2-Diacylglycerol 3-glucosyltransferase is associated with the membrane surface catalyzing the synthesis of the major nonbilayer-prone lipid α-monoglucosyl diacylglycerol (MGlcDAG) from 1,2-DAG in the cell wall-less *Acholeplasma laidlawii*. Phosphatidylglycerol (PG), but not neutral or zwitterionic lipids, seems to be essential for an active conformation and function of the enzyme. Surface plasmon resonance analysis was employed to study association of the enzyme with lipid bilayers. Binding kinetics could be well fitted only to a two-state model, implying also a (second) conformational step. The enzyme bound less efficiently to liposomes containing only zwitterionic lipids, whereas increasing molar fractions of the anionic PG or cardiolipin (CL) strongly promoted binding by improved association (k_{a1}), and especially a decreased rate of return (k_{d2}) from the second state. This yielded a very low overall dissociation constant (K_D), corresponding to an essentially irreversible membrane association. Both liposome binding and consecutive activity of the enzyme correlated with the PG concentration. The importance of the electrostatic interactions with anionic lipids was shown by quenching of both binding and activity with increasing NaCl concentrations, and corroborated *in vivo* for an active enzyme−green fluorescent protein hybrid in *Escherichia coli*. Nonbilayer-prone lipids substantially enhanced enzyme−liposome binding by promoting a changed conformation (decreasing k_{d2}), similar to the anionic lipids, indicating the importance of hydrophobic interactions and a curvature packing stress. For CL and the nonbilayer lipids, effects on enzyme binding and consecutive activity were not correlated, suggesting a separate lipid control of activity. Similar features were recorded with polylysine (cationic) and polyglutamate (anionic) peptides present, but here probably dependent on the selective charge interactions with the enzyme N- and C-domains, respectively. A lipid-dependent conformational change and PG association of the enzyme were verified by circular dichroism, intrinsic tryptophan, and pyrene-probe fluorescence analyses, respectively. It is concluded that an electrostatic association of the enzyme with the membrane surface is accompanied by hydrophobic interactions and a conformational change. However, specific lipids, the curvature packing stress, and proteins or small molecules bound to the enzyme can modulate the activity of the bound *A. laidlawii* MGlcDAG synthase.

Lipid bilayers are essential permeability barriers and the local environment for most membrane proteins. Anionic lipids are determinants in membrane protein insertion, translocation, and topology (*1*, *2*), and for the binding and anchoring of many surface-associating proteins (*3*). Certain fractions of nonbilayer-prone lipids are also typical (*4*), and these affect the packing properties in membrane bilayers and their constituent peripheral and integral proteins (*5*−*8*).

In the prokaryote *Acholeplasma laidlawii*, the MGlcDAG synthase (EC 2.4.1.157) transfers glucose from UDP-glucose to 1,2-diacylglycerol (DAG), yielding the nonbilayer-prone α-monoglucosyldiacylglycerol (MGlcDAG).[1] The MGlcDAG synthase (MGS) is involved in maintaining a certain surface charge density on the lipid bilayer (*9*, *10*). A consecutive reaction produces the major bilayer-forming α-diglucosyldiacylglycerol (DGlcDAG), catalyzed by the DGlcDAG

† We thank the Swedish Natural Science Research Council for financial support.

* To whom correspondence should be addressed. Telephone: +46 8 162463. Fax: +46 8 153679. E-mail: ake@dbb.su.se.

‡ Department of Biochemistry, Umeå University.

§ These authors contributed equally to this work.

|| Present address: Wallenberg Laboratory for Cardiovascular Research, Göteborg University, Göteborg, Sweden.

⊥ Stockholm University.

Biacore AB.

@ Present address: Department of Microbiology, Colorado State University, Fort Collins, CO 80523.

[1] Abbreviations: CHAPS, 3-[(3-choloamidopropyl)dimethylammonio]-1-propanesulfonate; CL, cardiolipin; CT, CTP:phosphocholine cytidylyltransferase; DGlcDAG, 1,2-diacyl-3-*O*-[α-D-glucopyranosyl-(1→2)-*O*-α-D-glucopyranosyl]-*sn*-glycerol; DO, dioleoyl; DOG, 1,2-dioleoylglycerol; EDC, 1-ethyl-3-[3-(dimethylamino)propyl]carbodiimide hydrochloride; GFP, green fluorescent protein; Glc, glucose; GT, glycosyltransferase; LUV, large unilamellar vesicles; MGlcDAG, 1,2-diacyl-3-*O*-(α-D-glucopyranosyl)-*sn*-glycerol; MGS, MGlcDAG synthase; PC, phosphatidylcholine; PE, phosphatidylethanolamine; PG, phosphatidylglycerol; PyrPG, 1-palmitoyl-2-pyrenedecanoylphosphatidylglycerol; RU, resonance units; SPR, surface plasmon resonance; UDP, uridine diphosphate.

10.1021/bi034360l CCC: $25.00
Published on Web 07/23/2003

synthase (EC 2.4.1.208). This enzyme is activated by phosphatidylglycerol (PG) and potentially interacting with the MGlcDAG synthase (*11*). These two glucolipids are major components for balancing the bilayer to nonbilayer phase equilibria (*12*), and for keeping a constant lipid bilayer spontaneous curvature (*13*).

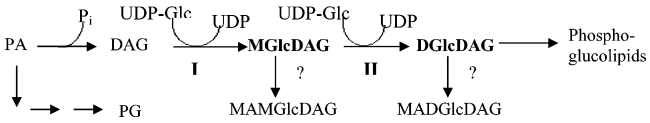

To transfer the water-soluble glucose to the hydrophobic substrate DAG embedded in the membrane, the enzyme should be membrane-associated with the active site facing the bilayer. The gene for the MGlcDAG synthase is functionally cloned (*14*). The encoded enzyme lacks a signal peptide and transmembrane segments, and is supposed to be located on the cytosolic side of the membrane. Ten to twenty mole percent of the negatively charged PG is necessary for the activity (*15*), and PG protected the enzyme from proteolytic digestion of the enzyme by proteinase K, possibly by orienting a lysine-rich face toward the membrane (*16*). A very high theoretical pI (9.5) was predicted, with a major contribution from the N-terminal half of the sequence (pI = 10) containing clusters of positively charged amino acids, while the C-terminal half yielded a lower pI (6.9). A three-dimensional fold prediction (*14*, *17*) revealed a similarity to the structure of the membrane-bound glycosyltransferase (GT) MurG from *Escherichia coli* (*18*) and a soluble GlcNAc-epimerase with an analogous structure (*19*). A potential membrane attachment by a positively charged amphipathic helix could be proposed (*14*). The C-terminal domain contains the conserved motif EX_7E for retaining α-glycosyltransferases belonging to CAZy family 4 of glycosyltransferases (*20*−*22*). Sequence similarity searches identified a group of related proteins with unknown functions in various pathogenic bacteria. Genes from two species were cloned and functionally shown to encode enzymes with a function identical or similar to that of the MGlcDAG synthase, including PG dependence (*14*, *23*).

Lipid GTs can be membrane-bound or soluble (*24*), and between these two states, several modes of surface attachment are possible (cf. ref *25*). An interplay of cationic and hydrophobic/aliphatic residues may yield vastly different membrane binding characteristics, like for certain phospholipases and kinases (*26*, *27*). From this, several important issues can be raised. (i) What are the mechanisms for interaction and association of the MGS enzyme with a lipid bilayer? (ii) How stable is the interaction? (iii) Are surface binding and activity separate events? (iv) Can other factors (or molecules) interfere with surface binding and activity? (v) Are there differences in the secondary or tertiary structure upon activation by PG? The results suggest that especially electrostatic but also hydrophobic interactions are involved, in a two-step process, in the tight binding and consecutive activation of the MGlcDAG synthase on the membrane surface. Most likely, the clusters of positively charged amino acid residues in the N-domain make the enzyme bind to the anionic lipids. In addition to activator and nonbilayer-prone lipids, other molecules with clusters of charges such as polylysine and polyglutamate peptides can also affect the binding and activity.

MATERIALS AND METHODS

Materials. The pET 15b vector and *E. coli* strain BL21-(DE3) were purchased from Novagen Inc. Synthetic *rac*-1,2-dioleoylglycerol (1,2-DOG) was from Larodan, and beef heart cardiolipin (CL), DOPG, and DOPC were from Avanti Polar Lipids. Sensor Chip CM5, Pioneer Chip L1, and the amine coupling kit were from Biacore AB). Poly(L-lysine) (MW > 4000) and poly(L-glutamic acid) (MW ∼ 1000) were from Sigma. 1-Ethyl-3-[3-(dimethylamino)propyl]carbodiimide hydrochloride (EDC) was from Pierce and *N*-(1-pyrene)maleimide from Molecular Probes.

Overexpression and Purification of the His-Tagged MGlcDAG Synthase. pET 15b was used for overexpression of the His_6-tagged MGlcDAG synthase. The gene was obtained by PCR amplification from the genomic DNA of *A. laidlawii* strain A-EF22 with primers 5′-GGTGGTCTCGAGGAAATCGAAGGTCGTATGAGAATTGGTATTTTTTCGGAAGCG-3′ and 5′-GGTGGTGGATCCTTACTTTTTATTCAATTTTTTGTTATTTTTATC-3′ (underlined bases are restriction sites for *Xho*I and *Bam*HI). The plasmid containing the MGlcDAG synthase gene was introduced into *E. coli* BL21(DE3). Cells were grown at 23 °C in 2× Luria-Bertani medium with 100 μg/mL ampicillin. Isopropyl thio-β-D-galactoside (0.3 mM) was added for induction when the absorbance at 600 nm reached 0.6. Cells were harvested after overnight induction at 23 °C. Plasmid isolation, restriction endonuclease digestions, DNA ligation reactions, transformation, and DNA sequencing were performed under the conditions recommended by manufacturers (Saveen, Pharmacia, Novagen, QIAGEN, and PE Applied Biosystems). Harvested cells were homogeneously suspended in buffer containing 20 mM HEPES (pH 8), 10% glycerol, 300 mM NaCl, 10 mM CHAPS, and 20 μM PMSF. After sonication for 3 × 10 s, the solution was stirred at 4 °C for 2 h. The supernatant with CHAPS-solubilized material was then collected after centrifugation at 20000*g* for 20 min. Three different chromatography techniques were used: ion exchange chromatography, hydroxyapatite chromatography (HAC) (without CHAPS in elution buffer), and affinity chromatography Ni−NTA resin for His-tagged protein. The first two column steps were carried out as described previously (*15*, *16*). The pooled fractions containing MGlcDAG synthase activity from HAC were mixed with Ni−NTA resin by mild shaking in the presence of 5 mM imidazole for 4 h. The Ni−NTA resin column was washed with 10 volumes of wash buffer containing 20 mM HEPES (pH 8), 300 mM NaCl, 10% glycerol, and 20 mM imidazole. The MGlcDAG synthase was eluted with 20 mM HEPES (pH 8), 300 mM NaCl, 10% glycerol, and 100 mM imidazole. All the procedures were carried out at 4 °C; glycerol and a low temperature are very important for enzyme stability over time. The samples were analyzed by activity assay, SDS−PAGE, and Western blot analysis using Penta His (QIAGEN) as the primary antibody.

Localization of MGlcDAG Synthase−GFP Fusion Variants. Full-size (398 amino acids), N-domain (amino acids 1−226), and C-domain (amino acids 227−398) MGlcDAG synthase were cloned upstream and in frame with the gene

for green fluorescent protein (GFP) using a PCR primer approach based on the enzyme sequence (*14*) and the vector pGFPuv (Clontech), in *E. coli* JM109. Ligation, transformation, and selection followed standard procedures, and the constructs that were obtained were verified by DNA sequencing. Enzymatic activities of the hybrid proteins were analyzed after induction with IPTG, by labeling of *E. coli* lipids *in vivo* with radioactive acetate (*14*), and by an assay for MGlcDAG synthesis after CHAPS detergent solubilization *in vitro* (*14*). Localization of the MGS−GFP variants in *E. coli* was analyzed by fluorescence microscopy after growth with 0.1 or 0.75 M NaCl supplements, using a Zeiss Axioplan2 microscope, FITC filters, a CCD camera (Sony), and Image Access 3.0 software (Imagic Bildverarbeitung AG).

Preparation of Large Unilamellar Vesicles (LUV). Lipids in 2:1 (v/v) chloroform/methanol solutions were mixed to different compositions, and dried under nitrogen gas and in a vacuum overnight. The dried lipids were hydrated with intermittent vortexing for 60 min in 250 μL of 10 mM HEPES (pH 8.0) with 5 mM $MgCl_2$, or in Biacore measurements with HBS-N [20 mM HEPES (pH 7.4) and 150 mM NaCl, filtered and deoxygenated] with 10% (v/v) glycerol. LUV were made by 19 successive extrusions of the lipid dispersions through double 100 nm polycarbonate filters (Millipore) by using a LiposoFast small volume homogenizer (Avestin). The LUV were stable for at least 1 week at 4 °C.

Enzyme Activity Assay. MGlcDAG synthase (25 μL) was added to 20 μL of the prepared liposomes (containing 3 mol % 1,2-DOG) in the presence of 5 mM $MgCl_2$ and kept on ice for 30 min. The enzyme reactions were started by adding 5 μL of 10 mM UDP-Glc mixed with 62.4 pmol of UDP-[^{14}C]glucose (37−74 GBq/mol). After incubation for 30 min at 28 °C, the reactions were stopped with a 2:1 (v/v) methanol/chloroform solution and lipids extracted and separated by thin-layer chromatography (*28*, *29*). The produced MGlcDAG was quantified by electronic autoradiography (Packard Instant Imager).

Real-Time Binding of Liposomes to MGlcDAG Synthase. A BIACORE 3000 instrument (Biacore AB), or a BIACORE 2000 instrument for the initial screening, was used to study real-time binding of 100 nm liposomes (analyte), at a concentration of ~2.8 nM (0.25 mM lipid), to a sensor chip CM5 surface to which approximately 1700 RU (1.7 ng/mm^2) of MGlcDAG synthase enzyme (ligand) was amino-coupled. The carboxymethyl-modified dextran polymer on sensor chip CM5 was activated with an injection of 0.2 M *N*-ethyl-*N*-[(dimethylamino)propyl]carbodiimide and 50 mM *N*-hydroxysuccinimide for 7 min. MGlcDAG synthase (10 μg/mL) was injected for 16 min, and the surface was then blocked with 0.9 M ethanolamine in 10% (v/v) glycerol for 7 min. Binding of the analyte results in an increase in the surface plasmon resonance (SPR) signal measured in refractive units (RU). A reference surface, used for simultaneous blank subtraction, did not bind liposome. The flow rate was set to 10 μL/min to minimize foretic and mass transfer effects. Running buffer (also used in liposome preparation) consisted of HBS-N [20 mM HEPES (pH 7.4) and 150 mM NaCl, filtered and deoxygenated] with 10% (v/v) glycerol. Regeneration was accomplished by two pulses of 10 μL of 20 mM CHAPS detergent in run buffer, at a flow rate of 30 μL/min, which brought the signal back to the stable baseline. Series with PG and CL liposomes were run over the same chip surface. New surfaces were prepared for the series with DAG and PE liposomes. Resulting sensorgram curves could only be well fitted to a two-state model using BIA evaluation 3.0 software (eqs 1−5). Besides revealing real-time binding, this technique avoids labeling procedures that might affect binding and time-consuming detection methods.

$$\mathrm{A} + \mathrm{B} \underset{k_{d1}}{\overset{k_{a1}}{\rightleftharpoons}} \mathrm{AB} \underset{k_{d2}}{\overset{k_{a2}}{\rightleftharpoons}} \mathrm{AB}^* \quad (1)$$

$$\mathrm{d[B]}t/\mathrm{d}t = -k_{a1}[\mathrm{A}][\mathrm{B}] + k_{d1}[\mathrm{AB}] \quad (2)$$

$$\mathrm{d[AB]}t/\mathrm{d}t = k_{a1}[\mathrm{AB}] - k_{d1}[\mathrm{AB}] - k_{d2}[\mathrm{AB}] + k_{d2}[\mathrm{AB}^*] \quad (3)$$

$$\mathrm{d[AB^*]}t/\mathrm{d}t = k_{d2}[\mathrm{AB}] - k_{d2}[\mathrm{AB}^*] \quad (4)$$

$$k_{d1}/k_{a1} \times k_{d2}/k_{a2} = K_D \quad (5)$$

where A is the analyte (liposome), B is the immobilized ligand (MGlcDAG synthase enzyme), and AB is the complex of the liposome and enzyme. AB* is the liposome−enzyme complex where a conformation change has taken place. The ratio between dissociation rate constant k_d (s^{-1}) and association rate constant k_a (M^{-1} s^{-1}) gives the equilibrium dissociation constant K_D (M).

Binding of the Enzyme Using Centrifugal Analysis. Other binding experiments were carried out by using NANOSEP filters (Pall Filtron). The MGlcDAG synthase was incubated with liposomes with varying PG contents for 30 min at 4 °C on ice. The samples were then centrifuged at 14000*g* to separate the free enzyme molecules from those bound to the liposomes using a 300K NANOSEP instrument, and the enzyme was analyzed by activity assay and SDS−PAGE.

Circular Dichroism Spectroscopy. CD measurements were taken on a CD6 spectrodichrograph (Jobin-Yvon Instruments SA) at 4 and 25 °C. The MGlcDAG synthase was dialyzed overnight in buffer containing 10 mM potassium phosphate (pH 8) and 10% glycerol. The concentration of the enzyme was 5 μM (with or without liposomes). All the spectra were recorded using a 0.5 mm quartz cell and corrected by subtracting the corresponding baselines.

Protein Fluorescence Analysis. For analysis of tryptophan emission, 50 μL of liposomes (1 mM lipid) with different compositions was mixed with MGlcDAG synthase or a melittin reference peptide to a protein:lipid molar ratio of 1:800 (MGlcDAG synthase enzyme) or 1:100 (melittin peptide) and incubated on ice (4 °C) for 30 min. Samples were analyzed at room temperature in a Perkin-Elmer LB50 spectrofluorimeter. Slit bandwidths were set to 10 nm; excitation was at 295 nm to exclusively excite tryptophan, and emission spectra were collected between 310 and 400 nm. Liposomes used in analysis of resonance energy transfer between tryptophan and pyrene contained 1 mol % PyrPG, and transfer was observed as an increase in the pyrene monomer emission between 360 and 400 nm, with peaks at 376 and 395 nm.

In separate experiments, the two cysteine residues in MGlcDAG synthase were labeled with pyrene (*30*). A 1:2 enzyme/DTT mixture was incubated for 2 h at 37 °C to reduce SH groups. A portion (25 μL, 18 nmol) of a mixture of 34 mmol of *N*-(1-pyrene)maleimide in DMSO was then

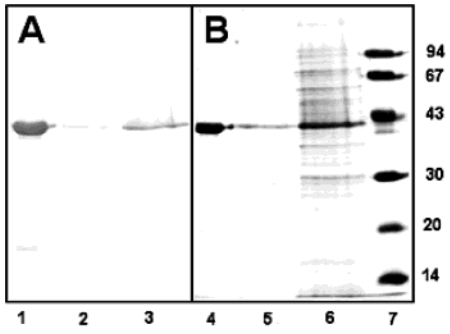

FIGURE 1: Purification of His-tagged MGlcDAG synthase. (A) Western blot of the SDS gel in panel B using Penta His as the primary antibody. (B) SDS gel stained with Coomassie Brilliant Blue (Materials and Methods). Lanes 1 and 4 and lanes 2 and 5 contained different fractions of the purified His-tagged MGlcDAG synthase from the final Ni−NTA column; lanes 3 and 6 contained CHAPS-solubilized *E. coli* cells, and lane 7 contained a commercial reference with molecular masses in kilodaltons. Note that there are no extra bands when the gel is overloaded (lane 4).

mixed with 4.44 nmol of enzyme previously reduced, and the mixture was incubated for 2.5 h at 37 °C in the dark. Gel filtration through a NAP5 column (Pharmacia) removed the unreacted pyrenemaleimide. The excimer:monomer ratio (I_e/I_m) for the attached pyrene probes was then measured at room temperature as the emission at 478 nm to that at 395 nm on a Spex Fluoromax-2 spectrofluorometer at an enzyme concentration of 0.5 μM. The MGlcDAG synthase:PG-detergent ratio was 1:100. Except for incubation and measurement, the enzyme was stored on ice. However, activity was eventually lost over time, as for labeling with N-(1-ethyl)maleimide.

RESULTS

Expression and Purification of the MGlcDAG Synthase. The MGlcDAG synthase gene from *A. laidlawii* (*14*) was ligated into plasmid pET 15b with a His_6 tag at the N-terminus, overexpressed, and purified from *E. coli* by three chromatography techniques (Materials and Methods). Figure 1 shows the purified enzyme by SDS−PAGE and Western blot analysis. The yield reached more than 2 mg/L of *E. coli* culture, and the enzyme remained soluble in buffer without detergent after purification (1−2 mg/mL).

Binding of the MGlcDAG Synthase to Liposomes. The mechanism for the regulation of the MGlcDAG synthase by PG is little understood, but the PG fractions in micelles and liposomes, not the total amount, are very important for the activation and conformational change of the enzyme (*15*, *16*). To resolve binding and activity, binding studies were carried out with an SPR-based BIACORE 3000 instrument. Initial screening to identify proper conditions made clear the fact that the enzyme is unstable over time at room temperature; 10% of binding capacity remained after 16 h, and there was no activity after 2 h. Using the MGlcDAG synthase as the analyte, there was unspecific binding to the anionic dextran matrix of the chips. The Ni surface of the NTA sensor chip immobilized the enzyme properly by binding to the His tag at the N-terminus of the MGlcDAG synthase (data not shown), but no consecutive binding of PG-containing liposomes to the enzyme was detected. With this kind of coupling, all the enzymes were supposed to be uniformly oriented, which might hide or prevent access of the expected

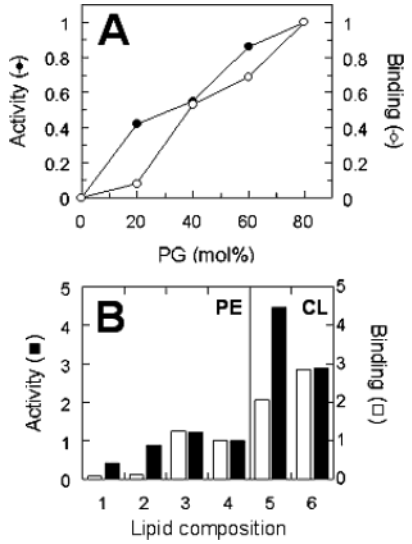

FIGURE 2: Binding and activity in liposomes containing different amounts of DOPG. (A) Liposomes at 0.57 nM (0.05 mM lipid) contained 5% DOG with different PG contents. DOPC was used as the matrix lipid, and was stepwise exchanged with DOPG. The data were normalized to the system with 80% DOPG. The MGlcDAG synthase was immobilized on sensor chip CM5 by amine coupling. (B) Binding and activity are modulated by other lipids. The liposomes contained 5% DOG with different DOPG, CL, and DOPE contents, and DOPC as the matrix lipid. Liposomes at 11.4 nM (1 mM lipid) were injected over the surface with bound enzyme: (1) 20% DOPG, (2) 20% DOPG and 10% DOPE, (3) 20% DOPG and 30% DOPE, (4) 80% DOPG, (5) 20% CL, and (6) 60% CL.

membrane binding sites of the enzyme. However, immobilizing the enzyme by amino coupling on a CM5 surface gave an orientation allowing binding of liposomes. Initial studies showed that both the anionic lipids PG and CL, and the nonbilayer-prone lipid PE, could promote activity and binding (Figure 2). A correlation between the level of binding and activity was observed for PG (Figure 2A); this was not the case for PE, where the level of binding increases more than activity, or CL, where a greater amount bound leads to decreased activity (Figure 2B). Analysis of the binding of the native MGlcDAG synthase, purified from *A. laidlawii*, to liposomes with different PG contents by a filter centrifugal separation technique (Materials and Methods) yielded similar results (data not shown). Thus, proper conditions for the binding study were immobilization of the MGlcDAG synthase enzyme on sensor chip CM5 by amine coupling, and different LUV preparations injected over the chip surface. Lipids where chosen to reflect the dependence of anionic and nonbilayer-prone lipids. Immobilizing the enzyme also circumvented the possibility of multimerization, indicated by the finding that the protein did not enter an SDS−PAGE gel when cross-linking had been performed in the presence of PG liposomes but not PC ones (data not shown).

Electrostatic Interactions Strongly Influence Association and Dissociation. An increased content of DOPG (Figure 3A) or CL (Figure 3B) in the liposomes induced an increased level of binding of liposomes to the enzyme. A very slow dissociation observed after the injection had stopped indicated strong binding. The curves could only be well-fitted with a two-state binding model, involving a conformational change, using the BIA evaluation 3.0 software (Materials and Methods). Other binding models (1:1 binding with or without

Table 1: Binding Constants for Anionic Liposomes Binding to alMGS Enzyme Using a BIACORE 3000 Instrument (See Materials and Methods)[a]

lipid composition[b]	k_{a1} (M^{-1} s^{-1})	k_{d1} (s^{-1})	k_{a2} (M^{-1} s^{-1})	k_{d2} (s^{-1})	K_D (M)	fit (χ^2)
100% DOPC	1.1×10^6	9.1×10^{-3}	9.1×10^{-3}	2.1×10^{-4}	1.5×10^{-10}	7.66
20% DOPG	7.0×10^6	8.4×10^{-3}	5.9×10^{-3}	3.6×10^{-5}	7.2×10^{-12}	6.80
40% DOPG	7.6×10^6	1.3×10^{-2}	7.5×10^{-3}	2.3×10^{-5}	5.0×10^{-12}	9.48
60% DOPG	6.5×10^6	8.4×10^{-3}	6.4×10^{-3}	2.3×10^{-8}	4.6×10^{-15}	5.03
10% CL	5.8×10^6	1.6×10^{-2}	7.9×10^{-3}	6.1×10^{-5}	2.1×10^{-11}	8.36
20% CL	6.0×10^6	1.1×10^{-2}	6.6×10^{-3}	1.8×10^{-5}	4.9×10^{-12}	7.07
30% CL	5.3×10^6	1.1×10^{-2}	7.0×10^{-3}	4.4×10^{-9}	1.3×10^{-15}	9.45

[a] Curve fits were made to a two-state model using BiaEval 3.0 software. Constants k_a, k_d, and K_D are explained in Materials and Methods. χ^2 is a measure in resonance units of the average deviation between the fitted curve and experimental data. [b] DOPC lipid was the balance.

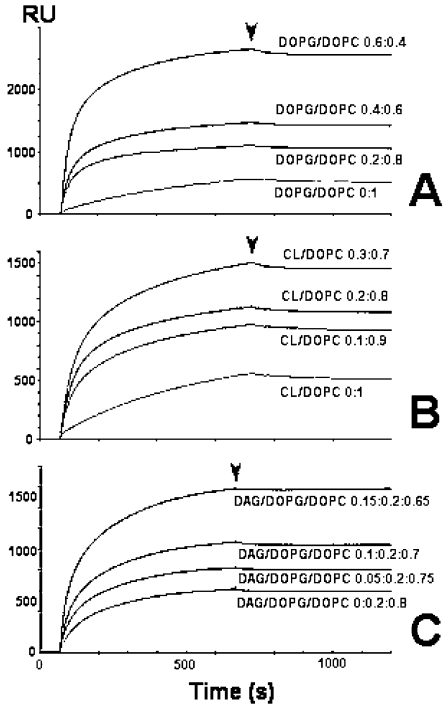

FIGURE 3: Binding of liposomes to the enzyme. Real-time binding, using a BIACORE 3000 instrument, of liposomes to surface-immobilized MGlcDAG synthase (see Materials and Methods). Liposome compositions are stated as mole fractions of the respective lipids. Liposomes at 2.8 nM (0.25 mM lipid) were injected over the surface. Arrows mark the end of injection. Resulting sensorgrams were well fitted only to a two-state model using BIA evaluation 3.0 software. The level of binding increased with an increasing amount of DOPG (A), CL (B), or 1,3-DOG (=DAG) (C).

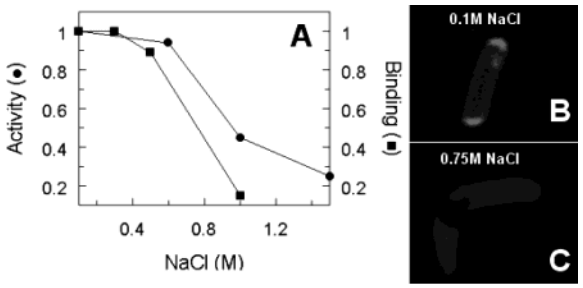

FIGURE 4: Quenching of binding and activity by NaCl. (A) Liposomes (1 mM) containing 60% DOPG were immobilized on pioneer chip L1 (with alkyl chains). Samples of 20 μg/mL MGlcDAG synthase together with different NaCl concentrations were injected over the sensor surface. Enzyme activities were measured as described in Materials and Methods. The data were normalized to the system containing 150 mM NaCl. (B and C) Images from fluorescence microscopy, where binding of a MGlcDAG synthase−GFP hybrid in *E. coli in vivo* is impaired by a high NaCl concentration (C) but binds to the cytoplasmic side of the plasma membrane at a physiological salt concentration (as in panel B).

mass transfer limitation, bivalent analyte, or heterogeneous ligand) produced very poor fits. The effect of the anionic lipid was an increase in the rate of association between the liposome and enzyme (k_{a1}, Table 1) and the maintenance of the enzyme in an active conformation via a decrease in the second dissociation constant (k_{d2}, Table 1). The smaller k_{d2} might reflect membrane insertion or specific interaction with the anionic lipid, as indicated for the C2 domain of phospholipase C (*31*) or the C1 domain of protein kinase C (*32*). The K_D was decreased by several orders of magnitude. This can partly be due to multiple interactions between the relatively large liposomes and a protein-dense sensor surface. However, the stronger binding correlated fairly well with the amount of negatively charged phosphate headgroups at the bilayer surface, which would be expected to be in surplus over the enzyme already at the lower concentrations. The enzyme also bound appreciably to neutral (zwitterionic) DOPC membranes. Furthermore, the sensorgram curve form and binding constants were very similar at different densities of enzyme on the surface, from 1700 RU down to 287 RU, and the mass of bound liposome decreased accordingly (data not shown). These facts indicate that multiple enzyme interactions are less likely to be the dominating mechanism for the observed changes in the dissociation rate.

Nonbilayer Lipids Strongly Enhance Binding. Binding and activity of the enzyme were enhanced when nonbilayer-prone lipid DOPE or DOG was mixed with 20% DOPG in DOPC liposomes, compared to 20% DOPG only (Figure 3C). The effect of nonbilayer-prone lipids on binding was not as much to enhance association as to decrease the rate of the second dissociation step (k_{d2}, Table 2). Hence, this property plus the headgroup of PG or CL was very stimulatory for enzyme localization and function.

Salt Screens the Binding of MGlcDAG Synthase to Membrane. Liposomes containing 60% DOPG (anionic) were immobilized on the L1 chip surface (with alkyl chains), and the binding of the MGlcDAG synthase ("cationic") was analyzed in the presence of different concentrations of NaCl as a charge quencher (Figure 4A). The level of binding of the MGlcDAG synthase to the liposomes decreased in an obvious manner with increasing NaCl concentrations, corresponding to a loss of enzyme activity (Figure 4A). This is typical for electrostatically surface-bound proteins or peptides not attached by strong hydrophobic interactions (*3*, *33*). From native *A. laidlawii* membranes, ~50% of the MGlcDAG synthase activity was released by a high-NaCl wash, and even more by chaotropic reagent KSCN (ref *34* and data

Table 2: Binding Constants for Liposomes, Containing Nonbilayer-Prone Lipids, Binding to alMGS Enzyme Using a BIACORE 3000 Instrument (See Materials and Methods)[a]

lipid composition[b]	k_{a1} (M^{-1} s^{-1})	k_{d1} (s^{-1})	k_{a2} (M^{-1} s^{-1})	k_{d2} (s^{-1})	K_D (M)	fit (χ^2)
0% DOG/PE	3.1×10^6	7.8×10^{-3}	1.0×10^{-2}	4.6×10^{-5}	5.4×10^{-12}	1.2
5% DOG	5.4×10^6	1.3×10^{-2}	1.0×10^{-2}	2.2×10^{-5}	5.0×10^{-12}	0.80
10% DOG	5.5×10^6	1.1×10^{-2}	9.1×10^{-3}	6.7×10^{-9}	1.5×10^{-15}	0.70
15% DOG	7.1×10^6	1.6×10^{-2}	9.6×10^{-3}	9.3×10^{-9}	2.2×10^{-15}	10.3
10% DOPE	1.4×10^6	5.0×10^{-3}	2.5×10^{-2}	9.1×10^{-5}	1.4×10^{-11}	3.5
20% DOPE	3.5×10^6	9.0×10^{-3}	8.6×10^{-3}	1.4×10^{-8}	4.3×10^{-15}	0.67
30% DOPE	5.5×10^6	1.5×10^{-2}	9.3×10^{-3}	8.2×10^{-9}	2.3×10^{-15}	1.6

[a] Fits were made according to a two-state model using BIA Eval 3.0 software. [b] All liposomes contained 20 mol % DOPG, and DOPC was the balance. For an explanation of the constants and fit, see the footnotes of Table 1.

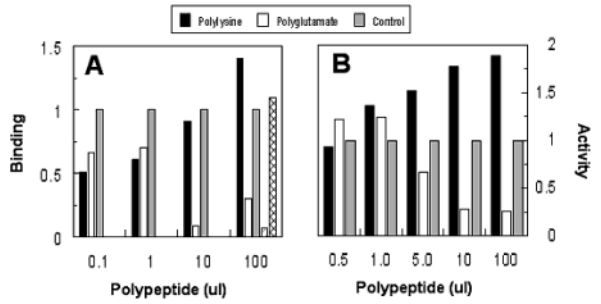

FIGURE 5: Effects of charged peptides on the MGlcDAG synthase. Liposomes (1 mM) containing 60% DOPG (DOPC as a balance) were immobilized on pioneer chip L1 in a BIACORE 2000 instrument. (A) Polypeptides at different concentrations were mixed with MGlcDAG synthase (final concentration of 22.5 μg/mL) and then injected over the L1 surface. (B) The activity measurements in the presence of the additives were carried out as described in Materials and Methods. Polylysine (black bars), polyglutamate (white bars), binding of polylysine to 60% PG liposomes (gray bars), and (first) binding of polylysine followed by (second) enzyme to 60% PG bilayer (cross-hatched bars). The data are normalized to the samples without peptides.

not shown). Liposomes (0.6:0.4 DOPG/DOPC) bound to enzyme on the sensor chip CM5 surface could only partially (~20% of mass) be removed by 0.65 M NaCl in the running buffer (data not shown), indicating that a hydrophobic component is also important for the binding. In addition, an *in vivo* high salt concentration screens the membrane interaction of an enzymatically active hybrid between MGlcDAG synthase and cytoplasmic green fluorescent protein (GFP), as revealed by fluorescence microscopy (Figure 4B,C). Growth of *E. coli* with high external NaCl concentrations yields correlated increases in the intracellular Na^+ concentration (*35*), which here prevented enzyme−membrane association (Figure 4C). Corresponding analyses with the N- and C-domains fused to GFP (Materials and Methods) localized the membrane binding activity to especially the (cationic) N-domain of MGlcDAG synthase, but not the (anionic) C-domain (Figure 6 in ref *17*). The native GFP (without partners) was properly localized to the cytoplasm (*17*), in agreement with its net negative charge.

Binding and Activity Are Affected by Charged Polypeptides. The binding of the MGlcDAG synthase depends on the negative charge of the bilayer matrix and the ionic strength of the environment (above). Will other molecules with different charges affect this process? Here, the negatively charged polyglutamate and positively charged polylysine were used to study how peptides potentially affect the function of the MGlcDAG synthase (Figure 5). Low concentrations of polylysine inhibited both the binding of the MGlcDAG synthase to liposome membranes and the consecutive activity of the enzyme. A competition between the enzyme and polylysine for binding to the negatively charged membranes might cause the inhibition at low concentrations. Surprisingly, a strong stimulation was achieved when a high concentration of polylysine was mixed with the enzyme. Polylysine itself could bind neither extensively nor tightly to the membrane as seen from the experiments shown in Figure 5A. It may be proposed that an interaction between polylysine and the negatively charged C-terminal half of the MGlcDAG synthase promotes binding of the enzyme. Note that a correspondence between the binding and activity of the MGlcDAG synthase was always present with polylysine (Figure 5).

Negatively charged polyglutamate was expected to compete with the negatively charged membranes for enzyme binding. At a low concentration of polyglutamate, certain PG-binding sites on the enzyme may be occupied by polyglutamate. The membrane binding was inhibited slightly, while the activity was enhanced somewhat (Figure 5). Other small molecules with several negative charges, like EDTA and EGTA at low concentrations, were also found to be able to stimulate the activity of the MGlcDAG synthase in the presence of activator lipid PG (data not shown). However, high concentrations of the polyglutamate peptide strongly inhibited both binding of the MGlcDAG synthase to the membrane and its activity.

Conformational Changes of the MGlcDAG Synthase. PG can protect the enzyme from proteolytic digestion by proteinase K, whereas PC could not (*16*), suggesting a conformational or orientational change of the MGlcDAG synthase by the presence of the activator lipid. The Biacore binding kinetics indicated a conformational change upon membrane binding of the MGlcDAG synthase, which was different depending on the content of PG or CL (Table 1), or nonbilayer lipid (Table 2). CD spectra supported a structure change when the lipid composition was varied (Figure 6). Liposomes with only 20% PG yielded a minor change, whereas a substantial change occurred with 30% PE. However, the spectra of the MGlcDAG synthase with 80% PG liposomes in the presence of 1 M NaCl looked similar to those with DOPC liposomes, or in buffer. Most importantly, the spectra are typical for mixed α/β structures, and the lipid-induced changes yielded only minor differences in the secondary structure of the enzyme, similar to those recorded for the *E. coli* SRP receptor FtsY binding to liposomes (*36*). Further support for a conformational change in the enzyme was provided by fluorescence analysis of extrinsic and intrinsic fluorophores. First, the predicted three-dimensional structure of MGlcDAG synthase (*17*) proposes

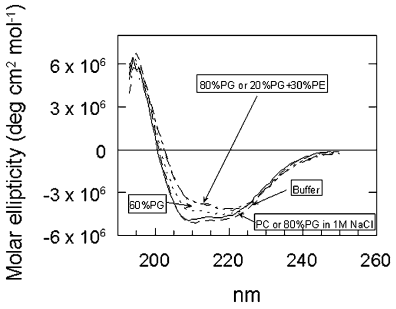

FIGURE 6: Circular dichroism analysis of the MGlcDAG synthase with different liposome compositions. The spectra were recorded using 5 μM MGlcDAG synthase in 10 mM potassium phosphate buffer (pH 8) and a lipid-to-protein molar ratio of 10. Baseline spectra were subtracted in the different systems.

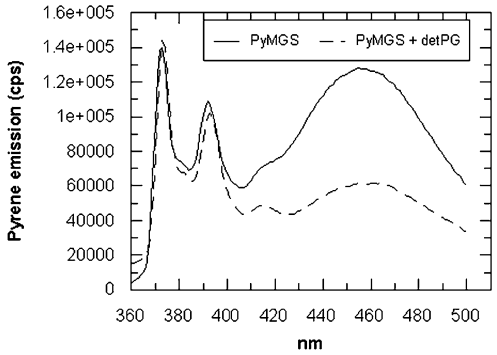

FIGURE 7: Pyrene labeling of the two cysteine residues in the MGlcDAG synthase. The two cysteines in the enzyme were labeled with pyrene to probe the intramolecular vicinity of these positions in the sequence (see Materials and Methods), i.e., whether they are close in space. The fluorescence emission from the pyrenes in 0.5 μM enzyme indicates a very short distance (<10 Å) between the cysteine positions, as revealed by the strong excimer emission (I_e) at 476 nm in comparison to the monomer emission (I_m) at 395 nm. Furthermore, addition of PG-detergent micelles (*16*) decreases the magnitude of the excimer signal, indicating that the positions move apart from each other and that the enzyme thus changes conformation upon binding.

that the two cysteines, C155 and C380, are close (~10 Å) in space (cf. Figure 9 below), and the excimer signal at 476 nm was strong for the pyrene-labeled cysteines in the MGlcDAG synthase (Figure 7). These positions then move apart when binding to detergent-PG micelles, as indicated by decreased I_e/I_m. Second, the only tryptophan in the MGlcDAG synthase (W59), on the potential binding surface, exhibited a distinct red shift with increased amounts of PG, CL, or 1,3-DOG, in parallel with increased emission intensity (Figure 8A). The established membrane-binding melittin peptide was used as a control, and its tryptophan spectra showed a blue shift and increased emission intensity, as well as energy transfer to a PyrPG lipid probe labeled at the acyl chain tail (ω-carbon) (Figure 8B), indicative of a hydrophobic membrane environment. The W59 in MGlcDAG synthase showed no energy transfer to the PyrPG probe, but its emission curve looked like that for melittin with 100% DOPC vesicles, indicating an interfacial location. Table 3 lists emission data extracted from Figure 8A.

Table 3: Emission Data Extracted from Figure 8A

	MGS		melittin	
lipid composition[a]	λ_{max}	intensity	λ_{max}	intensity
100% DOPC	347.50	24.2	353	25.4
20% DOPG	348	28.6	351.5	27.7
40% DOPG	355	37.7	343	32.2
20% CL	359	32.7	–	–
40% CL	364	58.6	–	–
20% CL and 8% DAG	360	39.9	–	–

[a] DOPC was used as a balance.

DISCUSSION

Binding of the MGlcDAG Synthase to a Lipid Bilayer Surface Is Irreversible. The SPR analysis technique has been employed to unravel several aspects of the activity for the MGlcDAG synthase from *A. laidlawii*, a key enzyme for the membrane bilayer/nonbilayer lipid balance and the lipid surface charge density. Binding of the enzyme to lipid bilayers containing biological fractions of anionic lipids is essentially irreversible under most conditions that were examined, and should *in vivo* not involve any shuttling between the cytoplasm and the membrane typical for nonresident proteins (cf. the introductory section and refs *3* and *25*). However, both binding and activity are strongly affected by local conditions.

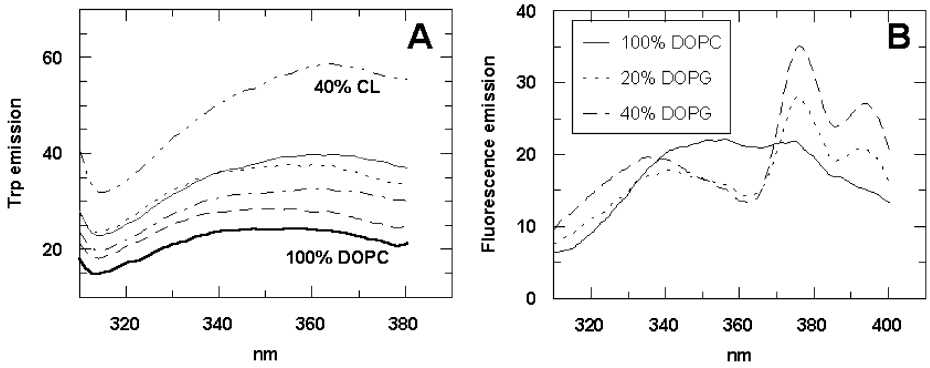

FIGURE 8: Intrinsic fluorescence of MGlcDAG synthase. (A) Fifty microliters of 1 mM liposomes was mixed with the MGS enzyme at a protein:lipid ratio of 1:800. Samples were excited at 295 nm, and emission was collected between 310 and 400 nm: (bold solid line) 100 mol % DOPC, (– – –) 20 mol % DOPG, (- - -) 40 mol % DOPG, (– - –) 20 mol % CL, (– - - –) 40 mol % CL, and (faint solid line) 20 mol % CL and 8 mol % 1,3-DOG. A red shift was evident when the amount of charged or nonbilayer-prone lipids was increased. (B) Fifty microliters of liposomes at a concentration of 1 μM lipid, containing 1 mol % PyrPG lipid (PG lipid with a pyrenedecanoyl chain in the *sn*-2 position), was mixed with the melittin reference peptide at a protein:lipid ratio of 1:100. Samples were excited at 295 nm, and emission was collected between 310 and 400 nm. Resonance energy transfer is evident between Trp in the peptide and the PyrPG lipid as a function of DOPG content. In addition, a blue shift in Trp emission can be observed. No energy transfer could be seen between W59 in MGS and PyrPG, but the curve looked like that for 100 mol % DOPC with melittin.

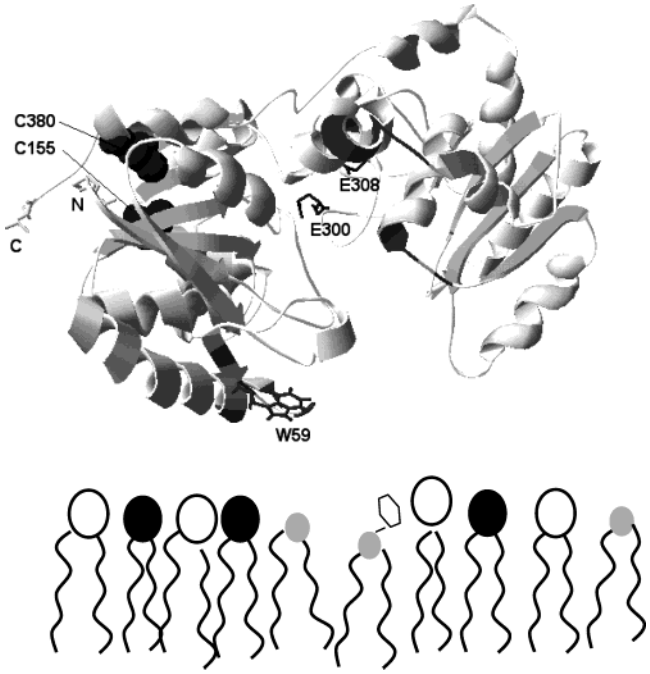

FIGURE 9: Interaction model. On the basis of a predicted and validated structure model (*17*) and available data from this work, an interaction model is proposed. The calculated pI values of the N- and C-terminal domains are 10 and 6.9, respectively. Binding is taking place at the basic surface of the N-terminal domain (to the left), where the exposed W59 residue and the amphipathic helix (bottom left) are located. Binding is augmented by the exposed hydrophobic parts (dark shaded secondary structure elements) of the C-terminal domain, predicted using MPEx [Jaysinghe, S., Hristova, K., and White, S. H. (2000) http://blanco.biomol.uci.edu/mpex]. The active site is in the cleft between the two domains, where the conserved E300 and E308, most likely involved in binding the UDP-Glc, are located. The cysteines, C155 and C380, are depicted as space-filled. Binding and activation are accompanied by a conformational change, probably involving orientation at the surface and penetration by hydrophobic parts.

(i) Binding Is Strongly Influenced by Anionic Lipids. The MGlcDAG synthase binds stronger to liposomes with an increasing content of anionic lipid DOPG (Figures 2A and 3A and Table 1) or CL (Figures 2B and 3B and Table 1), with almost no dissociation. Another effect seems to be to "lock" the enzyme in an active conformation (decreased k_{d2}, Table 1). The association constant is comparable to that of PLA_2 ($\sim 10^6$ M^{-1} s^{-1}) (*26*, *37*) but lower than that for the PKC β-II C2-domain (*38*, *39*), which seems to associate at the diffusion limit of 7×10^9 M^{-1} s^{-1}. However, the dissociation rate for MGlcDAG synthase is much lower than for PLA_2 ($\sim 10^{-4}$ s^{-1}) and for the PKC β-II C2-domain ($\sim 10^{-3}$ s^{-1}). A dissociation constant of $< 10^{-5}$ s^{-1} is at the limit of the Biacore technique, and lower values should only be interpreted as rough estimates. A high concentration of NaCl greatly inhibited binding to PG-containing liposomes (Figure 8A) and to the *E. coli* plasma membrane *in vivo* (Figure 8B), but only a fraction could be removed with an elevated NaCl concentration once the enzyme had bound (data not shown). Compared with that of the MGlcDAG synthase, dissociation of the polylysine peptide from PG-containing membranes was substantial on an L1 surface containing PG (data not shown). Polylysine cannot penetrate into the polar headgroup region of a lipid bilayer because of interactions between the lysine residues and anionic lipids (*33*).

A local increase in the PG concentration in a bilayer, caused by domain formation due to a chain length mismatch according to pyrene−PG probe data, is strongly stimulatory for the DGlcDAG synthase activity in a corresponding manner (*40*). Concomitantly, the degree of acyl chain ordering is increased for domain PG (*40*). An analogous packing of PG here, i.e., 30 or 40% DOPG in PC bilayers with 18:1c, 16:1c, or 14:1c chains, caused a stepwise decrease in the level of liposome−MGlcDAG synthase binding and the corresponding activity (data not shown) with an increasing level of PG domains, just the opposite of the DGlcDAG synthase activity. Hence, a tighter packing of PG may prevent a stable bilayer interaction of the MGS enzyme.

(ii) Binding Is Strongly Enhanced by Nonbilayer-Prone Molecules. Binding was better with an increasing level of nonbilayer-prone lipid 1,3-DOG (Figure 3C and Table 2) or DOPE (Figure 2B and Table 2). The effect on the binding constants is above all to decrease the k_{d2}, locking the enzyme in a changed conformation. The presence of even fairly small amounts of nonbilayer-prone molecules yielded a substantially enhanced binding of the enzyme. This was most prominent for CL and most likely because of an additional contribution from its headgroup charges (cf. above). Improved binding as an effect of nonbilayer-prone lipids occurs also for several surface-associating proteins such as protein kinase C (*3*, *41*, *42*) and the cytidylyltransferase (*3*, *43*−*45*), and was explained for the latter as a release of curvature elastic (chain packing) stress by the partial insertion of an amphipathic helix. Indeed, the level of acyl chain order in liposomes decreases with binding of the MGlcDAG synthase, while it increased in the presence of nonbilayer-prone lipids (*46*). Most likely, the charge interactions between the enzyme and the membrane were strengthened by hydrophobic interactions caused by surface packing defects or release of lateral stress caused by DOPE, DOG, or CL (cf. refs *43* and *45*). It should be noted that the consecutively acting DGlcDAG synthase is even more stimulated by nonbilayer-prone lipids than the MGlcDAG synthase (*47*).

(iii) Binding Is Modulated by Charged Polypeptides. The binding of the enzyme is not only dependent on the properties of the membranes. Results with the soluble polypeptides (Figure 5) indicate a complex regulation of the MGlcDAG synthase *in vivo*. The MGlcDAG synthase can bind to both cationic and anionic ion-exchange chromatography matrices while the enzyme has a net positive charge at pH 8 (A. Dahlqvist, unpublished data), presumably the polarized distribution of the positive and negative charges along the molecule. A substantial binding of the soluble enzyme to the dextran−COO^- surface of the CM5 and L1 chips occurs in the absence of covering lipids (data not shown). An enzyme−polylysine complex with an increased net positive charge will better bind to negatively charged membranes. Negatively charged polyglutamate can interact with the positively charged N-terminal domain of the MGlcDAG synthase, and therefore, the level of lipid binding will be decreased.

(iv) Activity Depends on the Bilayer Lipid Environment. Since binding was stable with little release of enzyme (Figure 3), a bound enzyme seemed to yield activity, but only residual if no PG or CL was present. However, at low DOPG or CL fractions (Figure 2), the specific activity was larger compared to when substantially more enzymes were bound at larger CL or DOPE fractions. Likewise, the presence of

small amounts of both soluble peptides substantially decreased the level of enzyme binding, while full activity was retained or even increased (Figure 5). It can thus be concluded not only that activity of the enzyme depends on membrane binding per se but also that the enzyme must adopt a certain conformation or orientation, and activity can be substantially modulated by interaction with various charged lipids or soluble molecules. Thus, anionic and nonbilayer-prone lipids are needed for faster binding and binding in a proper orientation or conformation. That PG (negatively charged phosphate lipid) is needed for activity is supported by the fact that the K_M is the same, but V_{max} increases substantially, with an increasing mole percent of PG (*11*, *15*). The reason may be that especially the rate of the second step (k_{d2}), dissociation, is decreased (Table 1).

Many amphitropic proteins bind to lipid bilayers in a *two-step process* (*3*): (i) an electrostatic pull to and interaction with anionic lipids followed by (ii) hydrophobic interactions and intercalation of certain segments (amphiphilic helices) in the interface. Binding strength is often determined by dissociation rates (*3*). The MGlcDAG synthase is predicted to have a structural two-domain organization, and a charge distribution similar to that of the MurG glycosyltransferase of the *E. coli* inner membrane (*14*, *18*). Figure 9 shows the validated prediction of MGlcDAG synthase structure (modified from ref *17*).

Likely candidate sequence segments for the attachment, besides the electrostatic interaction by the basic N-domain, are an amphipathic, positively charged helix (Figure 9, bottom left) and more hydrophobic, exposed segments in the C-domain (Figure 9, shaded gray). The two-step bilayer binding process found here for the MGlcDAG synthase by SPR binding analysis has also been found for Equinatoxin II and involves a conformational change (*48*). Analogously, the MGlcDAG synthase may bind first with the positively charged N-domain and second with hydrophobic parts in the C-domain. This is supported by the similarity in the N-region (MGS amino acids 40−75) to the amphipathic binding motifs for *E. coli* division protein MinD (*49*), the MurG glycosyltransferase (*18*), which seems to bind CL (*50*), and the PS-, PG-, and CL-binding motifs (*51* and references therein) present in various eukaryotic proteins. Once the enzyme is bound, the orientation and accompanying activity may be affected by the type of lipids in the bilayer, as for the amphiphilic cobra cardiotoxin (*52*).

Conclusions. This study provides evidence for the MGlcDAG synthase binding to membranes in a two-step process. The binding is faster and stronger by electrostatic attraction, but hydrophobic interactions are also involved in enhancing the binding and activation process. Once the enzyme is bound to the membrane, it is practically "glued" in an irreversible fashion, with no release. It also seems evident that the MGlcDAG synthase needs to bind in a proper orientation or conformation to be active. The consecutive activity is affected by the local lipid and molecular environment potentially influencing the orientation of the enzyme.

ACKNOWLEDGMENT

We thank Viola Tegman for excellent technical assistance and Professor Mikael Oliveberg for valuable discussion of CD spectra.

REFERENCES

1. von Heijne, G. (1992) *J. Mol. Biol. 225*, 487−494.
2. van Voorst, F., and de Kruijff, B. (2000) *Biochem. J. 347* (Part 3), 601−612.
3. Johnson, J. E., and Cornell, R. B. (1999) *Mol. Membr. Biol. 16*, 217−235.
4. Rilfors, L., Lindblom, G., Wieslander, Å., and Christiansson, A. (1984) in *Membrane Fluidity* (Kates, M., and Manson, L. A., Eds.) pp 205−245, Plenum Publishing Corp., New York.
5. de Kruijff, B. (1997) *Nature 386*, 129−130.
6. Booth, P. J., and Curran, A. R. (1999) *Curr. Opin. Struct. Biol. 9*, 115−121.
7. Booth, P. J., Templer, R. H., Meijberg, W., Allen, S. J., Curran, A. R., and Lorch, M. (2001) *Crit. Rev. Biochem. Mol. Biol. 36*, 501−603.
8. Botelho, A. V., Gibson, N. J., Thurmond, R. L., Wang, Y., and Brown, M. F. (2002) *Biochemistry 41*, 6354−6368.
9. Christiansson, A., Eriksson, L. E., Westman, J., Demel, R., and Wieslander, Å. (1985) *J. Biol. Chem. 260*, 3984−3990.
10. Karlsson, O. P., Dahlqvist, A., Vikström, S., and Wieslander, Å. (1997) *J. Biol. Chem. 272*, 929−936.
11. Vikström, S., Li, L., Karlsson, O. P., and Wieslander, Å. (1999) *Biochemistry 38*, 5511−5520.
12. Lindblom, G., Brentel, I., Sjölund, M., Wikander, G., and Wieslander, Å. (1986) *Biochemistry 25*, 7502−7510.
13. Österberg, F., Rilfors, L., Wieslander, Å., Lindblom, G., and Gruner, S. M. (1995) *Biochim. Biophys. Acta 1257*, 18−24.
14. Berg, S., Edman, M., Li, L., Wikström, M., and Wieslander, Å. (2001) *J. Biol. Chem. 276*, 22056−22063.
15. Karlsson, O. P. (1997) Ph.D. Thesis, Department of Biochemistry, Umeå University, Umeå, Sweden.
16. Li, L., Karlsson, O. P., and Wieslander, Å. (1997) *J. Biol. Chem. 272*, 29602−29606.
17. Edman, M., Berg, S., Storm, P., Wikström, M., Vikström, S., Öhman, A., and Wieslander, Å. (2003) *J. Biol. Chem. 278*, 8420−8428.
18. Ha, S., Walker, D., Shi, Y., and Walker, S. (2000) *Protein Sci. 9*, 1045−1052.
19. Campbell, R. E., Mosimann, S. C., Tanner, M. E., and Strynadka, N. C. (2000) *Biochemistry 39*, 14993−15001.
20. Geremia, R. A., Petroni, E. A., Ielpi, L., and Henrissat, B. (1996) *Biochem. J. 318* (Part 1), 133−138.
21. Kapitonov, D., and Yu, R. K. (1999) *Glycobiology 9*, 961−978.
22. Campbell, J. A., Davies, G. J., Bulone, V., and Henrissat, B. (1997) *Biochem. J. 326* (Part 3), 929−939.
23. Östberg, Y. (2002) Ph.D. Thesis, Department of Molecular Biology, Umeå University, Umeå, Sweden.
24. Kates, M. (1990) in *Handbook of Lipid Research* (Kates, M., Ed.) Plenum Press, New York.
25. Goñi, F. M. (2002) *Mol. Membr. Biol. 19*, 237−245.
26. Gelb, M. H., Cho, W., and Wilton, D. C. (1999) *Curr. Opin. Struct. Biol. 9*, 428−432.
27. Cho, W., Bittova, L., and Stahelin, R. V. (2001) *Anal. Biochem. 296*, 153−161.
28. Dahlqvist, A., Andersson, S., and Wieslander, Å. (1992) *Biochim. Biophys. Acta 1105*, 131−140.
29. Wieslander, Å., and Rilfors, L. (1977) *Biochim. Biophys. Acta 466*, 336−346.
30. Sahoo, D., Narayanaswami, V., Kay, C. M., and Ryan, R. O. (2000) *Biochemistry 39*, 6594−6601.
31. Ananthanarayanan, B., Das, S., Rhee, S. G., Murray, D., and Cho, W. (2002) *J. Biol. Chem. 277*, 3568−3575.
32. Ho, C., Slater, S. J., Stagliano, B., and Stubbs, C. D. (2001) *Biochemistry 40*, 10334−10341.
33. Ben-Tal, N., Honig, B., Peitzsch, R. M., Denisov, G., and McLaughlin, S. (1996) *Biophys. J. 71*, 561−575.
34. Karlsson, O. P., Dahlqvist, A., and Wieslander, Å. (1994) *J. Biol. Chem. 269*, 23484−23490.
35. Nagata, S., Adachi, K., Shirai, K., and Sano, H. (1995) *Microbiology 141* (Part 3), 729−736.
36. de Leeuw, E., te Kaat, K., Moser, C., Menestrina, G., Demel, R., de Kruijff, B., Oudega, B., Luirink, J., and Sinning, I. (2000) *EMBO J. 19*, 531−541.
37. Stahelin, R. V., and Cho, W. (2001) *Biochemistry 40*, 4672−4678.

38. Nalefski, E. A., and Newton, A. C. (2001) *Biochemistry 40*, 13216−13229.
39. Murray, D., and Honig, B. (2002) *Mol. Cell 9*, 145−154.
40. Karlsson, O. P., Rytömaa, M., Dahlqvist, A., Kinnunen, P. K., and Wieslander, Å. (1996) *Biochemistry 35*, 10094−10102.
41. Johnson, J. E., Giorgione, J., and Newton, A. C. (2000) *Biochemistry 39*, 11360−11369.
42. Newton, A. C. (2001) *Chem. Rev. 101*, 2353−2364.
43. Attard, G. S., Templer, R. H., Smith, W. S., Hunt, A. N., and Jackowski, S. (2000) *Proc. Natl. Acad. Sci. U.S.A. 97*, 9032−9036.
44. Davies, S. M., Epand, R. M., Kraayenhof, R., and Cornell, R. B. (2001) *Biochemistry 40*, 10522−10531.
45. Drobnies, A. E., Davies, S. M., Kraayenhof, R., Epand, R. F., Epand, R. M., and Cornell, R. B. (2002) *Biochim. Biophys. Acta 1564*, 82−90.
46. Storm, P., Li, L., Kinnunen, P., and Wieslander, Å. (2003) *Eur. J. Biochem. 270*, 1699−1709.
47. Dahlqvist, A., Nordström, S., Karlsson, O. P., Mannock, D. A., McElhaney, R. N., and Wieslander, Å. (1995) *Biochemistry 34*, 13381−13389.
48. Hong, Q., Gutierrez Aguirre, I., Barlic, A., Malovrh, P., Kristan, K., Podlesek, Z., Macek, P., Turk, D., Gonzalez Manas, J. M., Lakey, J. H., and Anderluh, G. (2002) *J. Biol. Chem. 277*, 41916−41924.
49. Szeto, T. H., Rowland, S. L., Rothfield, L. I., and King, G. F. (2002) *Proc. Natl. Acad. Sci. U.S.A. 99*, 15693−15698.
50. van den Brink-van der Laan, E., Boots, J.-W. P., Spelbrink, R. E. J., Kool, G. M., Breukink, E., Killian, J. A., and de Kruijff, B. (2003) *J. Bacteriol. 185*, 3773−3779.
51. Okamoto, Y., de Avalos, S. V., and Hannun, Y. A. (2002) *J. Biol. Chem. 277*, 46470−46477.
52. Huang, W.-N., Sue, S.-C., Wang, D.-S., Wu, P.-L., and Wu, W.-g. (2003) *Biochemistry 42*, 7457−7466.

BI034360L